Corrosion Protection of Steel Using ZnNiP Electroless Coatings

ELENA IONELA NEACSU[1], VIRGIL CONSTANTIN[1]*, VASILE SOARE[2], PETRE OSICEANU[1], MIHAI V. POPA[1], ANA MARIA POPESCU[1]*

[1]"Ilie Murgulescu" Institute of Physical Chemistry of the Romanian Academy, 202 Splaiul Independentei, 060022,Bucharest, Romania

[2] National Institute of Research and Development for Non-Ferous and Rare-Metals, New Materials and Technologies, 102 Biruintei Blv., 077145, Pantelimon-Ilfov, Romania

Electroless Zn-Ni-P thin films deposited on low carbon steel from sulphate-citrate aqueous electrolyte at pH=9.5 were investigated. The microstructure of the coatings was studied by scanning electron microscopy (SEM), energy-dispersive X-ray spectroscopy (EDX) and X-ray diffraction (XRD). The high corrosion resistance of Zn-Ni-P alloy plated steel sheet was confirmed by the electrochemical measurements in 3.5% sodium chloride solution. The surface analysis of the thin film samples before/after corrosion was performed by X-ray photoelectron spectroscopy (XPS) in an attempt to understand the chemistry of the obtained thin films. The element distribution within the coatings before and after the corrosion was evaluated along with the binding energies of the elements. The incorporation of Zn in Ni-P thin film is proved for all initial samples to be as a mixture of Zn and ZnO/Zn(OH)$_2$. Nickel was demonstrated to exist as a mixture of oxidized states Ni^{2+} and Ni^{3+} andP exists in and organic form. A passive film of a mixture of zinc oxide and hydroxides of zinc and nickel was formed on the surface and prevented the Zn-Ni-P corrosion.

Keywords: Electroless platting, Zn-Ni-P alloy, microstructure, corrosion protective coatings, XPS analysis.

Zinc coatings provide the most effective and economical way of protecting steel against corrosion. The Zn coated materials are characterized by higher corrosion resistance in aggressive environment [1]. Corrosion resistance of coatings can also be enhanced by using a zinc alloy. The corrosion resistance of Zn-Ni alloys, more superior to that of the classical zinc deposits, made them to be largely applied sometimes replacing the Cd deposits whose qualities (corrosion resistance, ductility, weldability) could not be matched yet [2-5]. On the other side we must agree that Zn-Ni alloy is not entirely nontoxic and this is why its acceptance is not unanimous [6]. Although electroless Zn-Ni alloys have extensive application to industry due to their excellent wear and corrosion resistance, some ternary electroless alloys such as Zn-Ni-P have been developed to further enhance the properties and to meet more rigorous demands [7-9]. Electroless deposited Zn-Ni-P thin film was considered as a barrier film on a galvanic Zn or Zn-Ni sacrificial layer in a multi-component corrosion protective coating on steel [10]. The advantage of such barrier film would be the reduced electrode potential difference with the steel substrate. The phosphorous addition to zinc-nickel alloy was found to refine the microstructure and improve the corrosion resistance of the deposits [11]. As it was proved that the addition of Zn to the Ni-P alloy greatly enhances a number of properties, including the corrosion resistance, several researches have been carried out to characterize the structure, phase-composition and corrosion resistance of Ni-Zn-P deposited from different baths [12-14].

The approach adopted in this work is to develop an optimized electroless process for plating of Zn-Ni-P ternary thin film alloy with high nickel content on low carbon steel substrate; a nickel sulphate bath containing sodium hypophosphite as reducer was used. The morphology of this thin film and a detailed analysis of the chemical composition are performed by using scanning electron microscopy (SEM), energy dispersive X-ray spectroscopy (EDX) and X-ray diffraction (XRD). Also the corrosion resistance was evaluated by polarization electrochemical techniques. In order to determine the chemistry of elements in the Zn-Ni-P thin film before and after the corrosion process the X-ray photoelectron spectroscopy (XPS) was employed.

Experimental part

Preparation of Zn-Ni-P coatings

Taking into account our former experience [15-17] optimized Zn-Ni-P thin film was electroless deposited on low carbon steel substrate (C=0.0043 wt %) from an electrolyte containing 40 gL^{-1} $NiSO_4 . 7H_2O$, 10 gL^{-1} $ZnSO_4 . 7H_2O$, 10 gL^{-1} $NaH_2PO_2 \cdot H_2O$, 50 gL^{-1} NH_4Cl and 85 gL^{-1} $C_6Na_3H_5O_7 \cdot 5_{1/2} H_2O$ (sodium citrate). The bath temperature was kept constant at 97°C ±0.5°C. The deposition time was kept constant at 60 min and the bath *p*H was adjusted to the range 9.5 by adding NH_3 25% solution. All solutions were prepared with analytical grade reagents (obtained from Merck and Sigma-Aldrich) and triply distilled water. Special surface finishing was applied to the steel substrate before deposition. After deposition the samples were washed with distilled water and dried with hot air.

Coating characterization

The morphology of the obtained thin films was analyzed by scanning electron microscopy (SEM) using a Philips XL-30-SEM microscope equipped with an energy dispersive X-ray spectrometer (EDS). The accuracy of the measurements for the equipment used was rated as ±0.1 wt %. The crystalline structure of the as-deposited thin films was characterized by using an X-ray diffractometer (model DRON-2) with Cu-K_α-radiation. X-ray patterns are received by automatic recording with 0.03° scanning step and 2-3 s exposition per step. Surface analysis of the obtained thin films performed by X-Ray Photoelectron Spectroscopy (XPS) was carried out on Quantera SXM equipment, with a base pressure in the analysis chamber of 10^{-9} Torr. The X-ray source was Al K_α radiation (1486.6 eV, mono-chromatized) and the overall energy resolution is estimated at 0.65 eV by the full width at half maximum (FWHM) of the $Au4f_{7/2}$ line. In order to take into account the charging

* *email*: *popescuamj@yahoo.com, virgilconstantin@yahoo.com*

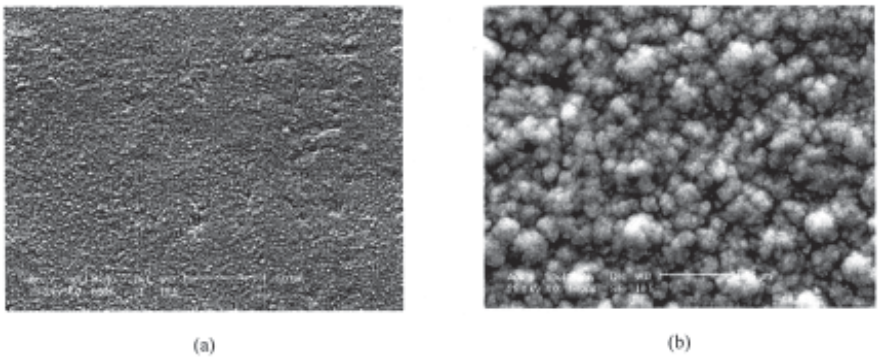

Fig.1. SEM images with ×500 (a) and ×5000 (b) magnification for the Zn-Ni-P thin film deposited on steel

effect on the measured Binding Energies (BEs) the spectra were calibrated using the C1s line (BE=284.8 eV, C-C $(CH)_n$ bondings) of the adsorbed hydrocarbon on the sample surface [18]. The deconvoluted peaks were identified by reference to an XPS data base [19, 20]. We have to emphasize that the errors in our quantitative analysis (relative concentrations) were estimated in the range of ±10%, while the accuracy for Binding Energies (B.Es) assignments was ±0.2 eV.

Polarization measurements

Electrochemical measurements for uncoated/coated steel samples were performed using a 3.5 wt % NaCl aerated aqueous solution under ambient conditions by using a Princeton Applied Research-USA, model PARSTAT 2273 potentiostat, with a "Power Corr" software. A thermostatic glass cell with a standard three electrode system was used, with the steel samples as the working electrode (WE), a saturated calomel electrode as reference electrode (SCE) and a platinum sheet (with a surface area greater than that of the WE) as the auxiliary electrode (AE). The cell assembly was located at a Faraday cage to prevent electrical interferences. To begin the experiments the sample was introduced into the cell and was allowed to reach equilibrium, which usually took around 20 min. The linear polarization curves at ±20 mV were collected starting from the open-circuit potential (OCP) after a constant value was achieved (up to 30 min) [21]. Tafel polarization experiments were performed with constant scan rate of 0.166 $mV \cdot s^{-1}$, while the potential was being shifted within ±250 mV *vs.* E_{OCP} [16].

Results and discussions

Surface morphology and elemental analysis of the deposits

The Zn-Ni-P thin film obtained was bright grey in appearance. The morphology of the film is shown in figure 1, showing a uniform, homogenous and not porous deposit, with round quasi-spherical grains (visible at higher magnification) which are compactly distributed on the surface of the coating.

The EDS spectra (fig. 2) contain mainly Zn, Ni, P elements with little amount of Fe and O, which demonstrate the purity of the studied thin films. The EDS analysis shows that the chemical composition of the studied samples is almost the same in different zones. The EDS spectrum/ analysis indicates a Ni-rich alloy (93.06 wt % Ni) with P (3.37 wt%) and Zn (3.57 wt%) incorporations.

Figure 3 shows the XRD pattern for the studied Zn-Ni-P thin film sample. The Cu K_α- radiation within $20^o \leq 2\theta \leq 100^o$ angle range contains four reflexes α-Fe (110), (200), (211), (220) of a large intensity which belong to cubic structure of Im$\bar{3}$m (229) space group with the unit cell parameter $a \approx 0.2866$ nm. This is in agreement with the data base 1998 JCPDS PCPDFWIN V.2, card N.06-0696. In $35^o \leq 2\theta \leq 57^o$ angle range the diffuse peak of X-rays dispersion by Zn-Ni-P coating respectively occurs. This diffuse peak has a FWHM $\Delta 2\theta \approx 8.044^o$ and its peak intensity in maximum is I ≈ 150 a.u. representing approximately 1/3 from peak intensity of (110) Fe reflex; the integral intensity of diffuse peak is $\Sigma_{film} \approx 1207.67$ that is almost 3 times more than integral intensity $\Sigma_{Fe} \approx 426.67$ of all observed iron peaks. The diffuse scattering peak of very small intensity occurs also in $70^o \leq 2\theta \leq 90^o$ angle range. The calculated grain size is $d_{cryst} \approx 6.41$ nm.

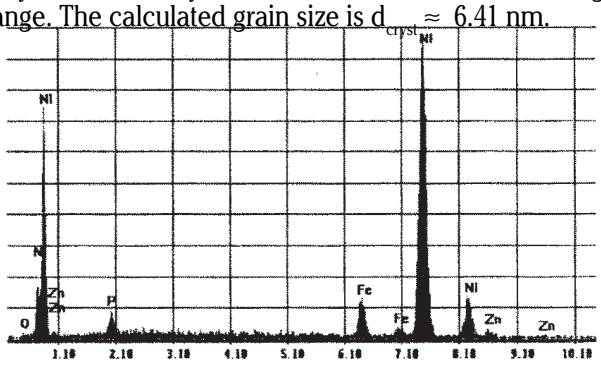

Fig.2. EDS spectrum of the Zn-Ni-P thin film deposited on steel

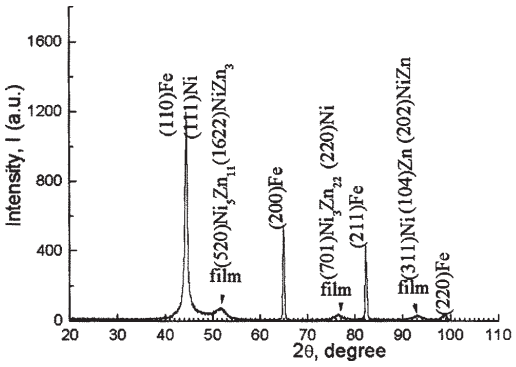

Fig.3 XRD pattern of the Zn-Ni-P thin film sample

Corrosion behaviour

Polarization tests were carried out to examine the effect of the thin films on the corrosion behaviour of the low carbon steel in 3.5 wt % NaCl aerated solution. The comparative OCP measurements *vs.* time for ZnNiP thin film coatings and for the steel substrate show a slow monotonous shift towards more positive values and after 1 h the OCP potential remain almost constant. At the initial time of immersion in the NaCl solution the studied thin films present OCP potential values from -0.539 V for uncoated steel (S) sample to -0.483 V for ZnNiP sample (table 1), hence this film cannot act as a sacrificial coating. The time evolution of OCP indicates that the passive film is thinning and consequently becomes vulnerable toward anion penetration of Cl^- ions. Also, we noticed slight oscillations of OCP in time which may probably result from chemical interactions between chloride ions and the structured

Sample	E_{OCP} [a] (V)	R_p [b] (Ω cm^{-2})	E_{corr} [c] (V)	i_{corr} [d] (A cm^{-2})	CR [e] (mm y^{-1})	IE [f] (%)
Uncoated steel (S)	-0.539	3.911	-0.706	8.960×10^{-6}	0.2104	-
ZnNiP	-0.483	769.34	-0.469	3.858×10^{-8}	0.0161	92.35

Table 1
CORROSION PARAMETERS MEASURED AND CALCULATED FOR THE STEEL SUBSTRATE (S) AND THE STUDIED ZnNiP THIN FILM IN 3.5 wt % NaCl SOLUTION, AT 30°C

[a]E_{OCP}= rest potential; [b]R_p=polarization resistance; [c]E_{corr}= corrosion potential; [d]i_{corr}= corrosion current density ; [e]CR=corrosion rate; [f]IE= inhibition efficiency, CR =corrosion rate of the steel support in absence (CR^0) and presence (CR^{sample}) of ZnNiP coating; $IE(\%) = \frac{CR^0 - CR^{sample}}{CR^0} \times 100$

Sample	Element composition (wt %)					
	C	O	Zn	Ni	P	Fe
$ZnNiP_{initial}$	23.68	7.63	2.48	63.97	2.21	-
$ZnNiP_{corroded}$ (after 120h)	18.61	18.39	2.65	36.87	0.84	22.64

Table 2
EXPERIMENTAL QUANTITATIVE XPS VALUES DETERMINED FOR THE INITIAL AND CORRODED ZnNiP COATING SAMPLE COMPOSITION.

passive film. As the Zn and Ni content in the thin films vary, it can be expected that the thin film having a higher amount of Ni to possess a higher corrosion resistance. Linear polarizations studies were carried out to estimate the polarization resistances (Rp) for corrosion of low carbon steel and of the various coatings studied. The resulting potential *vs.* current density curves shows a linear dependence. The slope of the linear part of these plots yields the polarization resistance values listed also in table 1. The Rp values obtained for Zn-Ni-P films are higher as compared to the steel substrate which means that these samples will have lower corrosion rate than the steel. Tafel polarization curves were also employed to evaluate the effect of the Zn-Ni-P thin film coatings on the corrosion resistance of carbon steel substrate.

Figure 4 shows the potentiodynamic polarization curves for the studied sample and the steel support. The corresponding corrosion parameters were presented in table 1 [22]. The Tafel plots indicate that the Zn-Ni-P thin film has better corrosion protective properties than the steel substrate. The sample shows a positive shift in the corrosion potential, which means a lower chemical activity than steel substrate and hence possess better chemical stability in the aggressive environment. The obtained results are in good agreement with the R_p values. Image introspection of samples after corrosion process confirm a low corrosion rate for the studied sample which has a good enough aspect after short-term corrosion test (48 h). In the same time the fine structure of the sample obtained by XRD measurements explains probably its high hardness [23]. We can conclude that deposits with high Ni content induce barrier properties thereby extending the life of the coatings

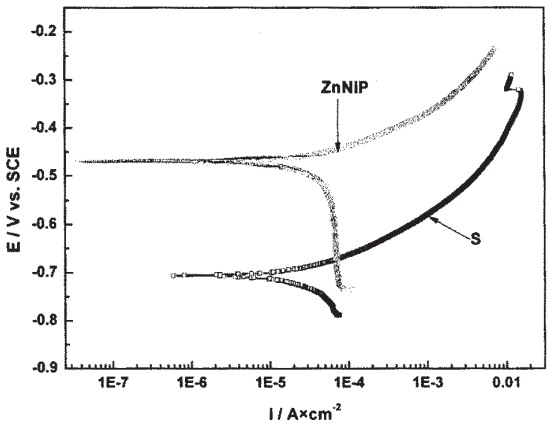

Fig.4. The comparative Tafel polarization curves of uncoated steel(S) and ZnNiP sample, in 3.5 wt. % NaCl solution at 30°C

XPS surface analysis before and after corrosion test

X-ray Photoelectron Spectrosopy (XPS) analysis was used to determine the chemical states of the elements present on the surface of the Zn-Ni-P thin film alloys deposited on steel substrate before and after the corrosion process. Survey (wide scan) XPS spectra were recorded to detect all the elements present on the surface (<10 nm). High resolution spectra were collected to find out the chemical bondings of the detected elements and for quantitative analysis, as well. Thus, the characteristic XPS spectra were recorded for the most prominent transitions: C1s, O1s, $Zn2p_{3/2}$, ZnLMM, $Ni2p_{3/2}$, P2p. The survey spectra for the studied sample before and after corrosion are

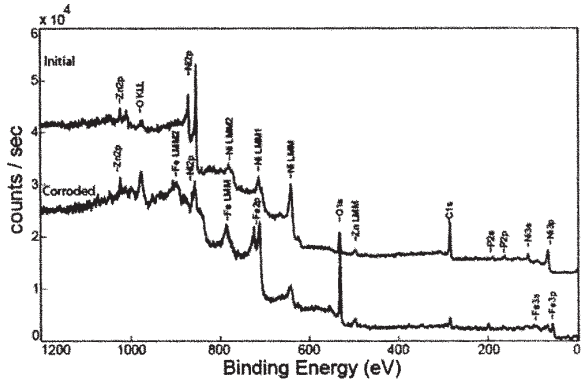

Fig.5. XPS survey spectrum for initial and corroded ZnNiP sample

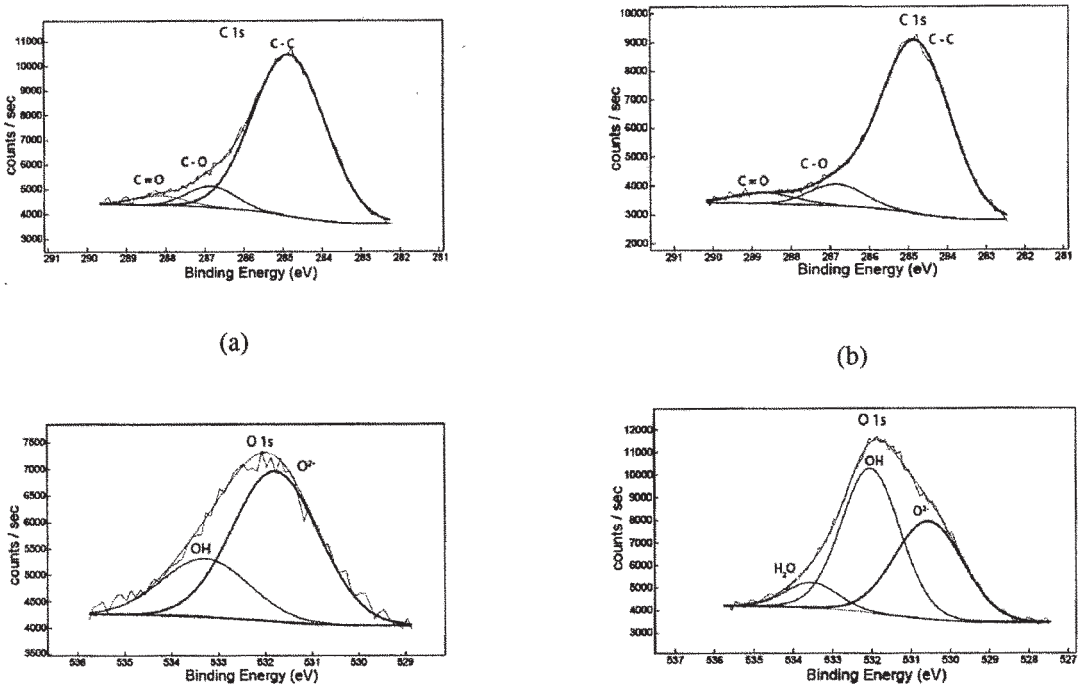

Fig.6. The peak deconvolution of narrow area spectra of the C and O in the initial (a, c) and coroded (b, d) state of the ZnNiP sample

Element / Sample	B.E. (eV)						
	Ni^0	NiO	Ni_2O_3	Ni	P	Zn	Zn
	$2p_{3/2,1/2}$	$2p_{3/2,1/2}$	$2p_{3/2,1/2}$	(satellites)	2p	$2p_{3/2}$	LMM
$ZnNiP_{(initial)}$	853.1	-	854.8	858.7	130.9	1022.1	497.9
	870.5	-	873.5	876.3	133.4	-	-
$ZnNiP_{(corroded)}$	853.2	855.0	858.3	861.1	133.6	1022.3	498.6
	870.6	873.4	876.0	879.4	-	-	-

Table 3
SUMMARY OF BINDING ENERGIES (B.ES.) FROM XPS ANALYSIS FOR THE INITIAL AND CORRODED ZnNiP SAMPLE

presented in figure 5. The contents of the deposits were calculated and listed in table 2.

After long term corrosion (samples exposed to 3.5 wt. % NaCl for period of 120 h) the surface chemistry of the sample shows significant changes by appearance of large amounts of Fe on the outermost surface layer.

By taking into account the errors in the quantitative analysis in both EDX and XPS methods the relative element concentrations (taking only Zn, Ni and P) for the studied sample are in good agreement (XPS values: 3.65% Zn, 93.10% Ni and 3.24% P). All elements decrease/drop abruptly, except Ni and Zn in the ZnNiP sample, which presents an increased resistance to the corrosion process. This result is in good agreement with electrochemical corrosion data. The characteristic thickness detected by XPS method for the deposited layers is found in the range of (5-8) nm.

From the calculated results, substantial amounts of C were detected on surface, which may be attributed to two sources. The surface is contaminated with unavoidable carbon from CO_2 and hydrocarbon adsorbed on the outermost layer from ambient atmosphere. Another reason is due to the presence of an organic compound (sodium citrate $C_6Na_3H_5O_7 \cdot 5 1/2\ H_2O$) used in the bath, which may have taken part in the formation of some complexes. Deconvolution data of C 1s spectra leads to the following bondings: C-C,C-O and C=O (fig. 6 a,b). The spectral O1s deconvolution (fig. 6 c,d) reveals the presence of O^{2-}, OH^- and a tiny amount of water (<2%). The detailed fitting results for the binding energies (BEs) of the main elements present in initial and corroded studied samples were summarized in table 3.

The Zn $2p_{3/2}$ and Zn LMM (Auger transition) spectra (fig. 7) indicate the presence of Zn^{2+} ion as ZnO in all of the films studied. Since it is practically impossible to detect a chemical shift between Zn^0 and Zn^{2+} states in the photoelectron line Zn $2p_{3/2}$, we recorded also the Auger LMM transition. Indeed only the ZnLMM Auger transition exhibits a chemical shift of ~2.5 eV to higher BEs for Zn in its 2^+ oxidation state as compared to Zn^0. From the Auger LMM transition it becomes clear that the inclusion of Zn in the initial stage of Zn-Ni-P electroless thin films is found to be in the 2^+ oxidation state as $ZnO/Zn(OH)_2$ (at binding energy of 498.0 eV). We attribute the existence of $ZnO/Zn(OH)_2$ from the $Zn2p_{3/2}$ spectra and corresponding binding energies of ~1022.7 eV for $Zn(OH)_2$ and ~1022.1 eV for ZnO . For the corroded samples (during ~96 h) the corrosion products of ZnNiP alloy platted steel was found to consist of zinc compound including $ZnO/Zn(OH)_2$ (at BE of 498.4 eV).

So, the Zn exists in oxidation state 2 on the surface of the Zn-Ni-P thin film in both initial and corroded sample. This result is in good agreement with former polarization measurements which proved that corrosion of zinc in oxygenated sodium chloride solution occurs by the anodic zinc dissolution and the cathodic oxygen reduction, with formation of Zn^{2+} and OH^-.

Because the solubility of $Zn(OH)_2$ is markedly low, zinc hydroxide precipitates on zinc surface and changes

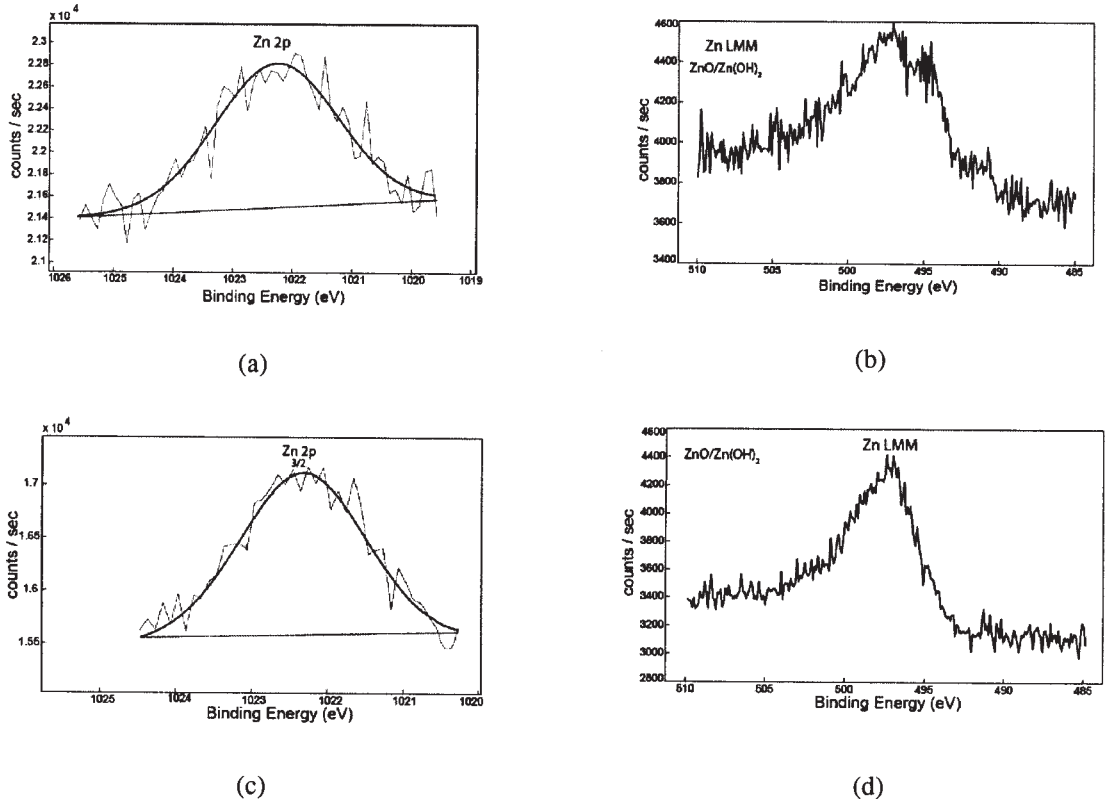

Fig.7. The peak deconvolution of narrow area for the initial and corroded ZnNiP sample : Zn2p (a,c) and Zn LMM (Auger transition)(b,d).

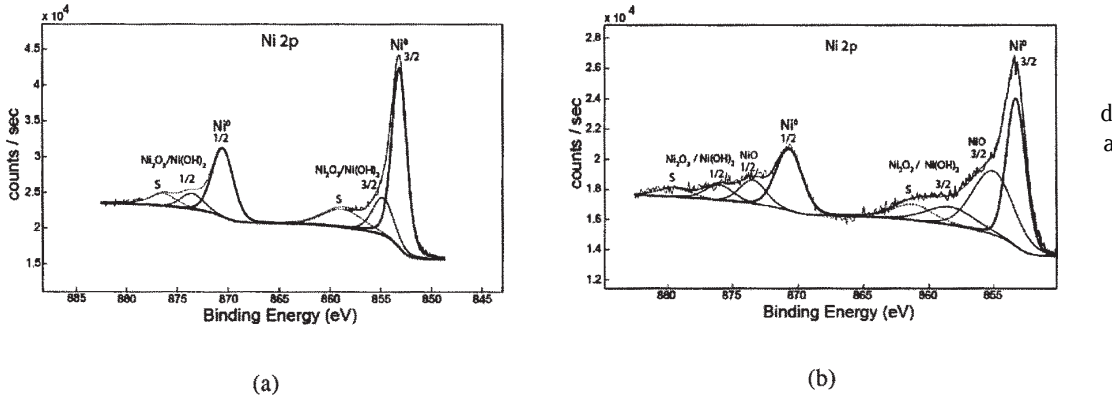

Fig.8. The peak deconvolution of narrow area spectra of Ni 2p for the initial (a) and corroded (b) ZnNiP sample.

gradually to ZnO. Thus, a passive film of a mixture of zinc oxide and hydroxide is formed on the surface and prevent the zinc corrosion. In the presence of chlorine ions the $Zn(OH)_2$ react with the chlorine ions to form soluble zinc oxychloride complexes [$ZnCl_2$. $Zn(OH)_2$], which can produce the local dissolution of the oxide passive film, resulting in pitting corrosion [21]. But in our case, the Cl^- was not detected by the XPS analysis, which indicates that Cl^- was not incorporated into the passive films explaining the good corrosion resistance of this sample.

The detailed XPS spectrum of nickel is presented in figure 8. The deconvoluted spectra for the initial ZnNiP sample, associated to nickel show the existence of a mixture of Ni^0, Ni^{3+} and Ni^{2+} chemical states from the line profile (including satellites) and the position of the Ni $2p_{3/2}$ peak.

The characteristic BEs of the 2p3/2 feature (853.1 eV; 854.8 eV), the band-like profile of the spectrum as well as the presence of the associated satelittes at 858.7 eV; 876.3 eV are the fingerprints of a mixture of NiO and Ni_2O_3/ $Ni(OH)_2$ contributions. The relative concentration of nickel in these two different chemical states is 40% Ni_2O_3 and 60% Ni^0.

The binding energies for Ni_2O_3 and $Ni(OH)_2$ are so close that they could not be quite separated, but it is already known that in sulfate baths Zn and Ni exist in the form of hydrated ions.

As for the corroded samples the deconvoluted XPS spectrum (fig. 8 b) shows additionally the appearance of NiO (BE 855.0 eV).

We can conclude that now it is clearly why this thin film having a good crystalline structure has such a good corrosion resistance, because both Zn and Ni are protected by a layer of oxide/hydroxide, which represent the protection of the steel support.

The detailed XPS spectrum of phosphorus P2p (fig. 9) is very noisy in the initial and corroded state of the sample as a result of the tiny relative concentation of this element in the Zn-Ni-P thin film; it shows two different peaks for the initial sample and only one peak for the corroded sample.

The first peak appears at a binding energy of ~130.1 eV and is detected as elemental phosphorus (P^0). The phosphorus signal at the binding energy of 133.6 eV can be assigned to an organic combination of phosphorous ($P_{organic}$) proving the expected citrate complexes in the deposition bath. After corrosionof the sample on the XPS spectrum only the organic P peak occurs. We can conclude that phosphorous do not participate in the corrosion process.

Finally, we can conclude that, on the dark grey surface, the enrichment of metal state nickel containing zinc corrosion product was observed after long term corrosion process. This means that the corroded surface is covered

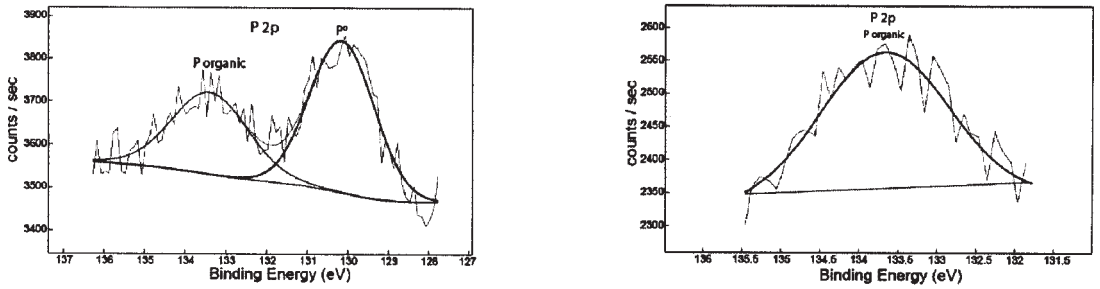

(a) (b)

Fig.9 The XPS deconvoluted spectra of phosphorous (P 2p) for the initial (a) and corroded (b) ZnNiP sample

with the oxide/hydroxide of zinc and nickel and because of the passivity by these layers, Zn-Ni-P alloy plated steel sheet shows much better corrosion resistance.

Conclusions

We successfully prepared a Zn-Ni-P thin film alloy on low carbon steel substrate by electroless deposition from sulfate-hypophosphite low alkaline bath. The thin film is compact, uniform and microcrystalline phases. EDS confirmed the formation of Zn-Ni-P coating with high Ni content (93.06 %). The XPS results demonstrated that the incorporation of Zn in the Ni-P electroless thin layer is possible in this electroless process. The inclusion of zinc is proved to be in an oxidized state, as a mixture of ZnO/ $Zn(OH)_2$. The phosphorus is proved to be in the elemental form as well as in an organic form, proving the existence of the citrate complexes in the bath. As for nickel, this was demonstrated to exist as a mixture of oxidized states Ni^{2+} and Ni^{3+}. The corrosion protection behaviour of these thin films on steel has been proved in 3.5% NaCl .

Acknowledgement. This work was carried out within the research programme "Molten Salts" of the "Ilie Murgulescu Institute" of Physical Chemistry, financed by the Romanian Academy and also financed by "EU(ERDF)-Romanian Government Program" that allowed the acquisition of the research infrastructure under POS-CEEO2.2.1 INFRANANOCHEM project-Nr.19/01.03.2009.

References

1. LI M.L., YANG C.F., LEE J.T., Corrosion, **47**, 1991, p.9.
2. SHIBUYA A., KURIMOTO T., KOREKEWA K., NOTI K., Tetsu-To-Hagane, **66,** 1980, p.71.
3. MUIRA N., SAITO T., KANAMARU T. SHINDO Y., KITAZAWA Y., Trans. Iron Steel Inst.Jpn., **23,** 1983, p.913.
4. LIN Y.P., SELMAN J.R., J. Electrochem. Soc., **140,** 1993, p.1299.
5. MIYOSHI Y., J. ISIJ Int., **31,** 1991, p.1.
6. BRENNER A., Electrodeposition of Alloys, New York and London,1963.
7. DURAIRAJAN A., KRISHNIYER A., POPOV B.N., HARAN B., POPOVA S.N., Corrosion, **56**, 2000, p. .283.
8. HUANG Y.S. , CUI F.Z., Acta Metall. Sinica, **18**, 2005, p.204.
9. WANG R., YE W., MA Ch., WANG Ch., Mater. Charact., **59**, 2008, p.108.
10. SCHLESINGER M., MENG X., SNYDER D., J. Electrochem. Soc., **138**, 1991, p.406.
11. SWATHIRAJAN S., MIKHAIL Y.M., US Patent 4 758 479, 1988.
10. VEERARAGHAVAN B., KIM H., POPOV B., Electrochim. Acta., **49**, 2004, p.3143.
12. HAMID Z.A., GHANEM W.A., ABO El ENIN S.A., Surf. Interface Anal., **37**, 2005, p. 792
13. WANG R., YE W., MA CH.,. WANG CH., Mater.Charact., **59**, 2008, p. 108
14. HAMID Z.A., Surf. Interface.Anal., **35**, 2003, p.496.
15. POPESCU A.M., CONSTANTIN V., SOARE V., TIRCOLEA M., OLTEANU M., Rev.Chim.(Bucharest), **62**, no. 9, 2011, p.899.
16. POPESCU A.M., CONSTANTIN V., OLTEANU M., SOARE V, BURADA M., NEACSU E.I., Rev.Chim.(Bucharest), **64**, no. 4, 2013, p.417
17.SOARE V., BURADA M., MITRICA M., CONSTANTIN I., STOICIU F., COTRUT C., POPESCU A.M., Metallurgy and New Materials Researches**, XIX (2),** 2011, p.33.
18. KANG H.B., BAE J.H., LEE J.W., PARK M.H., LEE Y.C., YOON J.W., JUNG S.B., YANG C.W., Scripta Materialia, **60**, 2009, p.257.
19. MOULDER J.F., STICKLE W.F., SOBOL P.E., BOMBEN K.D., Handbook of X-ray Photoelectron Spectroscopy, ULVAC-PHI Inc., Japan, 1995.
20. GROSVENOR A.P., BIESINGER M.C., SMART R.S.C., McINTYRE N.S., Surf. Sci., **600**, 2006, p.1771.
21. YANG L., Li J., ZHENG Y., JIANG W., ZHANG M., J. Alloy Compd., **467**, 2009, p.562.
22. REVIE R.W., UHLIG H.H., Corrosion and Corrosion Control-An Introduction to Corrosion Science and Engineering, 4 th.ed., John Wiley & Sons Inc., New York, 2008.
23. WANG S.L., CHIN. J., Appl. Chem., **21**, 2004, p.576.
24. ARAMAKI K., Corrosion Sci., **44**, 2002, p.871

Manuscript received: 23.04.2013